CrossMark

Comparison of the effect of land-sea thermal contrast on interdecadal variations in winter and summer blockings

Yongli He[1] · Jianping Huang[1] · Dongdong Li[1] · Yongkun Xie[1,2] · Guolong Zhang[1] ·
Yulei Qi[3] · Shanshan Wang[4] · Sonja Totz[5]

Abstract The influence of winter and summer land-sea surface thermal contrast on blocking for 1948–2013 is investigated using observations and the coupled model intercomparison project outputs. The land-sea index (LSI) is defined to measure the changes of zonal asymmetric thermal forcing under global warming. The summer LSI shows a slower increasing trend than winter during this period. For the positive of summer LSI, the EP flux convergence induced by the land-sea thermal forcing in the high latitude becomes weaker than normal, which induces positive anomaly of zonal-mean westerly and double-jet structure. Based on the quasiresonance amplification mechanism, the narrow and reduced westerly tunnel between two jet centers provides a favor environment for more frequent blocking. Composite analysis demonstrates that summer blocking shows an increasing trend of event numbers and a decreasing trend of durations. The numbers of the short-lived blocking persisting for 5–9 days significantly increases and the numbers of the long-lived blocking persisting for longer than 10 days has a weak increase than that in negative phase of summer LSI. The increasing transient wave activities induced by summer LSI is responsible for the decreasing duration of blockings. The increasing blocking due to summer LSI can further strengthen the continent warming and increase the summer LSI, which forms a positive feedback. The opposite dynamical effect of LSI on summer and winter blocking are discussed and found that the LSI-blocking negative feedback partially reduces the influence of the above positive feedback and induce the weak summer warming rate.

Keywords Land-sea thermal contrast · Blocking · Asymmetric warming · Double-jet

✉ Jianping Huang
hjp@lzu.edu.cn

1 Key Laboratory for Semi-Arid Climate Change of the Ministry of Education, College of Atmospheric Sciences, Lanzhou University, Lanzhou, Gansu 73000, China

2 State Key Laboratory of Numerical Modeling for Atmospheric Sciences and Geophysical Fluid Dynamics (LASG), Institute of Atmospheric Physics, Chinese Academy of Sciences, Beijing, China

3 School of Atmospheric Sciences, Chengdu University of Information Technology, Chengdu, China

4 Key Laboratory of Arid Climate Change and Reducing Disaster of Gansu Province and Key Open Laboratory of Arid Climate Change and Disaster Reduction of CMA, Institute of Arid Meteorology CMA, Lanzhou, Gansu, China

5 Department of Physics, University of Potsdam, Potsdam, Germany

1 Introduction

Atmospheric blocking, as the quasi-stationary anticyclones in the extra tropics, is an important weather system. It can induce large scale weather condition changes, particularly help the formation of extreme cold weather events and heat waves in various way. In summer, blocking prevails the descent flow and persists for few days or weeks, even over 1 month, confines the circulation and clear-sky radiative heating to severely increase the surface temperature. Examples include the 2003 European heatwave (Stott et al. 2004; Ogi et al. 2005; Tachibana et al. 2010), the 2010 Russian heat wave (Dole et al. 2011; Otto et al. 2012), which induces thousands of people died and billions of dollars

of economic loss. These heat waves have been reported to associate with the strong and long-lived blocking events. In winter, blocking is an important weather system that favors cold air advection from polar to mid-latitude and often induce large-scale severe cold events in the downstream of blocking, such as the Europe extreme cold weather event on the January–February 2012 (Luo et al. 2014a, b). Because blocking can threaten the lives and livelihoods of many people, particularly as extreme events are expected to increase the magnitude or frequency (Rahmstorf and Coumou 2011; Seneviratne et al. 2014; Sillmann et al. 2014), how atmospheric blocking is changing in the future is a question of great practical importance to societies.

Many theories have been proposed to describe the mechanisms associated the blocking dynamics not only from planetary scale (Egger 1978; Charney and DeVore 1979; Tung and Lindzen 1979; Kaas and Branstator 1993) but also local scale (Shutts 1983; Nakamura et al. 1997; Masato et al. 2012; Yamazaki and Itoh 2013). The formation and maintenance of blocking are not completely understood due to the highly non-linear characteristic. Planetary scale theories focus on statistic characteristic and consider the blocking as the linear resonance of planetary waves with surface thermal forcing and topographic forcing. Charney and DeVore (1979) emphasized the role of the zonal asymmetric thermal forcing in the transitions of zonal flow and wave-like flow. Shabbar et al. (2001) further investigated the relationship between the phase of North Atlantic Oscillation (NAO) and blocking frequency and persistence, found that in the positive phase of the NAO, the surface air temperature followed the "cold ocean/warm land" (COWL) pattern, which could decrease the blocking frequency and magnitude by reducing or destroying the resonant forcing of topography.

Under global warming since industries period, the continents in mid- and high-latitude experience the most enhanced warming, especially in winter season (Fu et al. 2006; Huang et al. 2012, 2016a, b; Wallace et al. 2012; Ji et al. 2014; Guan et al. 2015a, b). Due to the large differences of heat capacity, surface and boundary layer properties and cloud feedbacks over land and ocean (Sutton et al. 2007; Joshi et al. 2008; Dong et al. 2009), the rate of land warming is faster than that in ocean. Therefore, the land-sea thermal contrast has changed with global warming. He et al. (2014) demonstrated the changes of winter blocking and the land-sea thermal contrast under global warming could form a positive feedback to accelerate the warming progress. When the surface thermal forcing of Northern Hemisphere follows the "COWL" pattern due to CO_2 greenhouse effect, the zonally asymmetric thermal forcing starts to decrease, which reduces the blocking frequency and strength. At the same time, planetary waves in the mid-latitude are weaker and exert a weaker easterly wind forcing on the westerly wind. Thus, a stronger westerly reduces the meridional heating

exchanges and advects warming air from the oceans to the west of the continents to induce warming in these regions (He et al. 2014; Huang et al. 2016a). The additional warming associated with circulation changes further decreases the land-sea thermal contrast and forms the positive feedback. This feedback partially explains the asymmetry of the seasonal warming over mid-latitude. During the warming hiatus of 1998–2012, the Eurasian winter experienced a cooling trend (Kosaka and Xie 2013; Trenberth et al. 2014; Mori et al. 2014), which was related with the increasing blocking events (Li et al. 2015; Huang et al. 2016a) and might be the opposite process of above feedback.

However, to understand the asymmetric seasonal warming, the changes of summer blocking and its role in asymmetric seasonal warming progress compared with winter blocking should be investigated. Previous studies have investigated the summer blocking changes and summer land-sea thermal contrast changes, respectively. Arai and Kimoto (2008) suggested that a larger meridional temperature gradient between the Arctic Ocean and the Eurasian Continent enhances the polar frontal jet which becomes a wave guide of quasi-stationary Rossby waves. Increased Rossby waves breaking is one of the important factors to develop blocking anticyclones over the East Siberia and the Sea of Okhotsk (Nakamura and Fukamachi 2004). Kamae et al. (2014a, b) found that the land-sea thermal contrast in summer is increasing in recent decades and reveals in future climate projections. They demonstrated that the strengthening of land-sea contrast in summer could be attributed to the combination of the CO_2-induced positive and sea surface temperature (SST) induced negative contributions to the land-sea contrast. Shaw and Voigt (2015) found that the different circulation responses to direct radiative forcing and indirect sea surface temperature warming are directly connected to the opposite responses of land-sea thermal contrast to the two forcing components. When studying the influence of summer Northern Hemisphere annular mode (NAM) on 2003 abnormal summer heat wave, Ogi et al. (2005) found the summer NAM pattern could account for many of the anomalous weather features during the heat wave. During positive phase of summer NAM, double-jet streams and blockings support and extend periods of abnormal weather. The formation and maintenance of double-jet are associated with wave forcing of stationary and transient waves. Quasiresonant amplification (QRA) mechanism of planetary waves was further proposed to explain the recent Northern Hemisphere summer weather extremes (Petoukhov et al. 2013, 2016). They pointed out that persist high-amplitude zonal wave number m = 6, 7, 8 could trap the quasistationary free synoptic waves with zonal wave number k = m within relevant midlatitude waveguides, and favored a strong magnification of planetary wave amplitudes through resonance during summer extremes, or even 2 weeks before the onset of

events. They provided a possible mechanism for the increasing summer extremes, the combined effect of reduction of midlatitude westerly induced by weakened meridional temperature gradient associated sea ice loss and steepening of northern flank of the subtropical jet lead to a more frequent appearance of free wave with k = 6–8. However, the influence of the Arctic sea-ice on the Eurasian Continent has a big controversy. The recent "Warm Arctic, Cold Continents" pattern is suggested to be indeed forced by sea ice loss in winter (Inoue et al. 2012; Mori et al. 2014; Cohen 2016). Disagreement about summer extremes are related to Arctic warming and sea ice loss, Wu et al. (2016) pointed out that the greenhouse gas and SST warming outside the Arctic could explain nearly all land warming and sea ice loss could induce a negative Arctic Oscillation (AO) type circulation, which reduces the probability of regional summer extremes. However, as suggested by Charney and DeVore (1979), the zonal asymmetric thermal forcing plays an important role in the formation and maintains of blocking, which was not considered in Petoukhov's mechanism. Therefore, some details for summer blocking changes need further investigations.

Consistent with previous studies, seasonal warming has the very strong asymmetric characteristic, winter warming rate is much faster than summer during the accelerated warming period (1970s–1990s), especially in arid and semi-arid regions (Huang et al. 2012; Ji et al. 2014). In the future projections from different scenarios in the Coupled Model Intercomparison Project (CMIP5) experiments, the asymmetric warming in seasonal scale will be accelerated and induce accelerated expansion of drylands (Huang et al. 2016b). The feedback between decreased winter blockings and land-sea thermal contrast could partially explain the asymmetry of seasonal warming. However, whether there is a linkage between strengthening summer land-sea contrast and more frequent heat waves is still unclear. If the link exists, why the intensity of feedback in summer is weaker than winter? What does mechanism control the response of blocking to land-sea thermal contrast changes? These questions are critical for understanding the asymmetric seasonal warming phenomenon and predict the future blocking changes, and deserve further investigations.

The aim of this study is to investigate the influence of land-sea thermal contrast changes on blocking in winter and summer and to diagnose the role and mechanism of this relationship in the acceleration of seasonal asymmetric warming. Section 2 describes the data and the methods used in this study. Section 3 describes the land-sea thermal contrast changes in winter and summer. Section 4 outlines the circulation changes associated with land-sea contrast changes. Section 5 investigates the effect of land-sea contrast on summer and winter blocking. Section 6 identifies the actual mechanism resulting in different changes of summer and winter blockings and verifies the sensitivity of blocking to land-sea contrast by CMIP5 experiments. Finally, Sect. 7 summarizes and discusses the findings of this study.

2 Data and methods

The data used in this study includes the daily surface air temperature (SAT), geopotential height (GPH) and wind fields (zonal wind and meridional wind) and monthly GPH, sea level pressure (SLP) and wind fields of the NCEP-NCAR reanalysis from the Climate Diagnostics Center of the National Oceanic and Atmosphere Administration (NOAA). The resolution is $2.5° \times 2.5°$ horizontally with 17 levels in the vertical direction (Kalnay et al. 1996). It covers the time period from January 1948 to December 2015. The daily temperature, wind fields on 37 pressure levels from Japanese 55 year reanalysis (JRA-55) are used, which has a high spatial resolution ($1.25° \times 1.25°$) and covers 1958/01 to present (Kobayashi et al. 2015). We use December to February (DJF) mean for winter and June to August (JJA) mean for summer. The monthly mean SAT is obtained from the CRU, version TS3.23, which covers the period of 1901–2014 and has a horizontal resolution of $0.5° \times 0.5°$ (Mitchell and Jones 2005). The time series of monthly mean SST is provided by the Hadley Center for Climate Prediction and Research of the UK Met Office and covers the period of 1870 to present at a spatial resolution of $1.0° \times 1.0°$ (Rayner et al. 2003). Furthermore, the GISTEMP dataset from the National Aeronautics and Space Administration Goddard Institute for Space Studies (GISS) (Hansen et al. 2010) and the HadCRU4 dataset (Morice et al. 2012) are also used to compare the changes of land-sea thermal contrast. The time series of AO defined by Li and Wang (2003) (refer to AO_li) is obtained from the website (http://ljp.gcess.cn/dct/page/65607), the AO_li index is defined as the difference of the normalized monthly zonal-mean SLP between 35°N and 65°N. Traditional AO time series is obtained from Climate Prediction Center (http://www.cpc.ncep.noaa.gov/products/precip/CWlink/daily_ao_index/monthly.ao.index.b50.current.as.cii. table). The seasonally varying NAM (SVNAM) index is defined as the leading Empirical Orthogonal Function (EOF) modes performed for each individual month (Ogi et al. 2004), which is available on the website at http://wwwoa.ees.hokudai.ac.jp/people/yamazaki/SV-NAM/index.html.

3 Observed land-sea thermal contrast changes in winter and summer

To investigate the relationship between land-sea thermal contrast and blocking in summer, we first need define a land-sea index (LSI) to quantify the intensity of the zonal

asymmetric thermal forcing. Since all the theories about blocking including Charney's theory and Petoukhov's mechinism are essentially based on dry atmospheric dynamics (Pfahl et al. 2015), we only consider sensible heat differences between land and ocean, latent heat forcing is discussed in the Sect. 7. Because the LSI defined by net surface heat flux in the four key areas is similar to that defined by SAT, we define the LSI as a linear combination of the averaged SAT anomaly in the land and ocean between 30°N and 70°N, which is similar to previous studies (Molteni et al. 2011; Kamae et al. 2014a).

$$LSI = T\_ano[land,\ 30°N - 70°N] - T\_ano[ocean, 30°N - 70°N],$$

where T_ano is averaged SAT anomaly relative to the climatology of 1961–1990. Because of the difference of surface and boundary layer properties and cloud feedbacks over land and ocean, the warming rate in land is much faster than

ocean under global warming, no matter in winter or summer. Therefore, the positive LSI indicates a warmer climate and smaller land-sea thermal contrast in winter and larger land-sea thermal contrast in summer.

Figure 1 presents the time series of land-mean and ocean-mean SAT anomaly in the Northern Hemisphere (NH) extra-tropic (30°N–70°N) and their differences (land minus ocean) for winter and summer during 1901–2014. The result is similar when a different magnitude of averaged area is applied to the LSI definition (not shown). Clearly, the winter warming trend in land is 0.0151 °C/year, which is near twice than that in summer land. However, the winter warming trend in ocean (0.0059 °C/year) is nearly equal to that in summer ocean (0.0073 °C/year). Therefore, the LSI trend is dominated by the land warming trend, which is consistent with the result from HadCRU4 (Fig. S1) and GISS (Fig. S3) dataset. Due to the seasonal asymmetric warming, the LSI
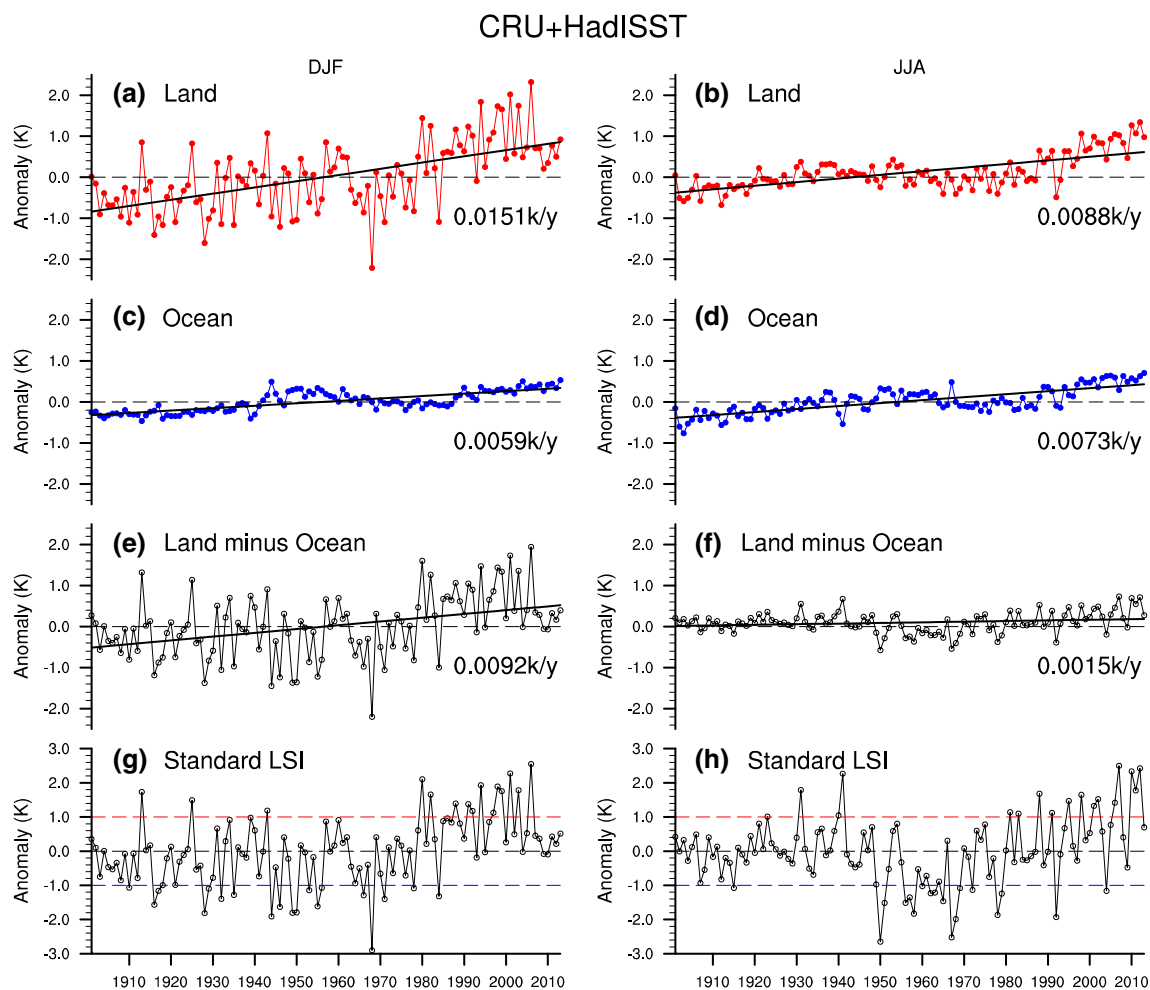

Fig. 1 Time series of winter (left) and summer (right) land-mean (**a, b**), ocean-mean (**c, d**) SAT and land-sea thermal contrast (**e, f**) averaged over the 30°N–70°N latitude belt. All values are anomalies relative to the climatology of 1961–1990. The lines and labeled values are linear trends (k/year) and all trends significantly exceed the 99% confidence level for two-side student's t test. **g** and **h** are the standard LSI during winter and summer, the red and blue reference lines indicate the ±1 standard deviation

trend in winter is 0.0092 °C/year, which is much more than that in summer. It is worth mentioning that the winter SAT has the different decadal variability with summer SAT. For example, in the second half of the twentieth century, the LSI in winter and summer are both increasing, but the LSI in winter shows a decadal deceasing trend after 2000s and the LSI in summer continued to increase (Fig. 1e, f). We also investigate the time series of the LSI without blocking events included as suggested by Luo et al. (2016) and the correlation coefficients between the LSI with and without blocking events included are 0.68 (winter) and 0.52 (summer) with 99% confidence level.

To further investigate the changes of land-sea thermal contrast, we compare the histograms of LSI in winter and summer during 1901–1940 and 1974–2013 based on the CRU and HadISST dataset (Fig. 2). In winter, the averaged LSI increased from −0.19 °C (1901–1940) to 0.52 °C (1974–2013), and the standard deviation does not change, which exceeds the 99% confidence level for the two-sided Student's test. In summer, the averaged LSI increases much more slowly than winter, from 0.11 °C to 0.21 °C and the

standard deviation of summer LSI during 1901–1940 is much smaller than that during 1974–2013 and does not exceed the statistical test with 90% confidence level, which indicates that the distribution of summer SAT is concentrated during 1901–1940. Different with winter, the standard deviation of summer LSI during 1974–2013 has a larger value, which favors more extreme events happen as expected in a warmer world (Rahmstorf and Coumou 2011). The similar results can also be seen from HadCRU4 (Fig. S2) and GISS (Fig. S4) dataset.

Consistent with previous studies (Kamae et al. 2014a, b), the thermal contrast between land and ocean in summer has gradually increased, especially since the 1980s. Based on the Charney-DeVore's equilibrium theory, the zonal asymmetric thermal forcing could influence the blocking frequency and strength by reducing or amplifying the resonance of planetary waves induced by thermal and topography forcing. Petoukhov's mechanism demonstrated that summer extreme events are induced by the amplified blocking. Although the land-sea thermal contrast has changed and is important for understanding the internal variability of atmospheric circulation in summer, few studies investigate the impact of land-sea thermal contrast changes on summer atmospheric circulation.

4 The associated atmospheric circulation changes

4.1 500 hPa GPH and SLP

To investigate the responses of atmospheric circulation to the change in the land-sea thermal forcing in summer, a regression analysis is carried out to measure the relationship between the land-sea thermal contrast and the circulation. Figure 3 shows the horizontal map of seasonal-mean 500 hPa GPH anomaly and SLP anomaly as regressed on the winter and summer LSIs from NCEP dataset. In winter, COWL pattern is very obvious in GPH regression field, which is discussed by many authors (Wallace et al. 1996; Wu and Straus 2004; He et al. 2014). Wallace et al. (1996) first named the "COWL" pattern and pointed out that the anomalous warming in the winters of the 1980s is induced by the strong positive anomaly of the COWL pattern. Wu and Straus (2004) redefined this pattern using the second EOF (empirical orthogonal function) of 500 hPa GPH and found that the mid-tropospheric temperature trend is mostly induced by COWL pattern. Figure 3e, f shows the regression map of SAT anomaly on the winter and summer LSIs from CRU and HadISST dataset. The result suggests that the winter LSI has a strong impact on the winter temperature in the continent, but the signal of summer LSI is much weaker than winter. He et al. (2014) demonstrated the feedback between COWL pattern thermal forcing and blocking could
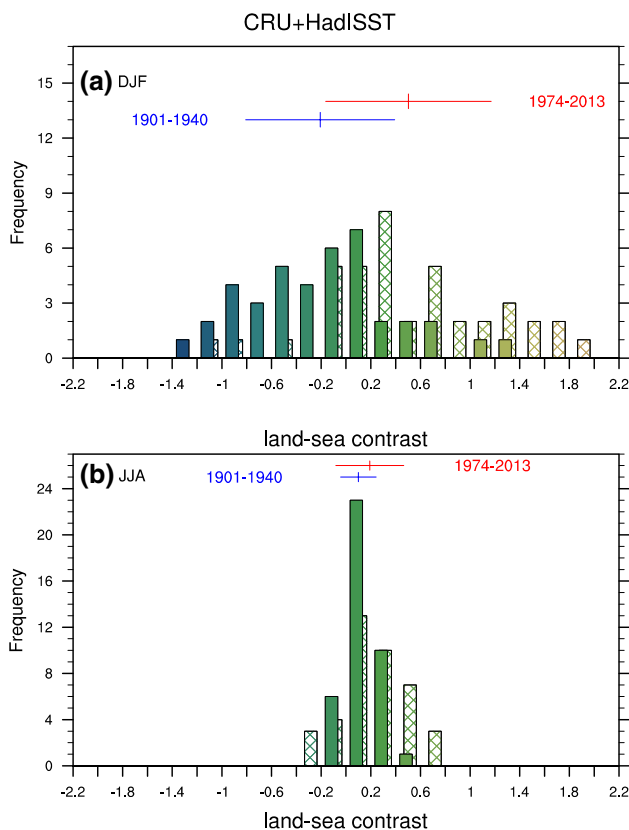

Fig. 2 Histograms of land-sea thermal contrast in winter (top) and summer (bottom) during two 40-year periods (1901–1940 and 1974–2013) based on the CRU and HadISST dataset. Units: K. Whickers in the upper part of the panels indicate the means and the ranges of ±1 standard deviations in the periods

Fig. 3 Horizontal maps of
500 hpa geopotential height
regressed on the winter LSI (**a**)
and the summer LSI (**b**) during
1948–2013. **c** and **d** As in **a** and
b but for SLP. **e** and **f** As in **a**
and **b** but for SAT. The units of
a and **b** are m, the units of **c** and
d are hpa, and the units of **e** and
f are °C. The dotted areas indi-
cate the regression coefficients
exceed the 99% confidence level

(a) GPH DJF

(b) GPH JJA

(c) SLP DJF

(d) SLP JJA

(e) SAT DJF

(f) SAT JJA
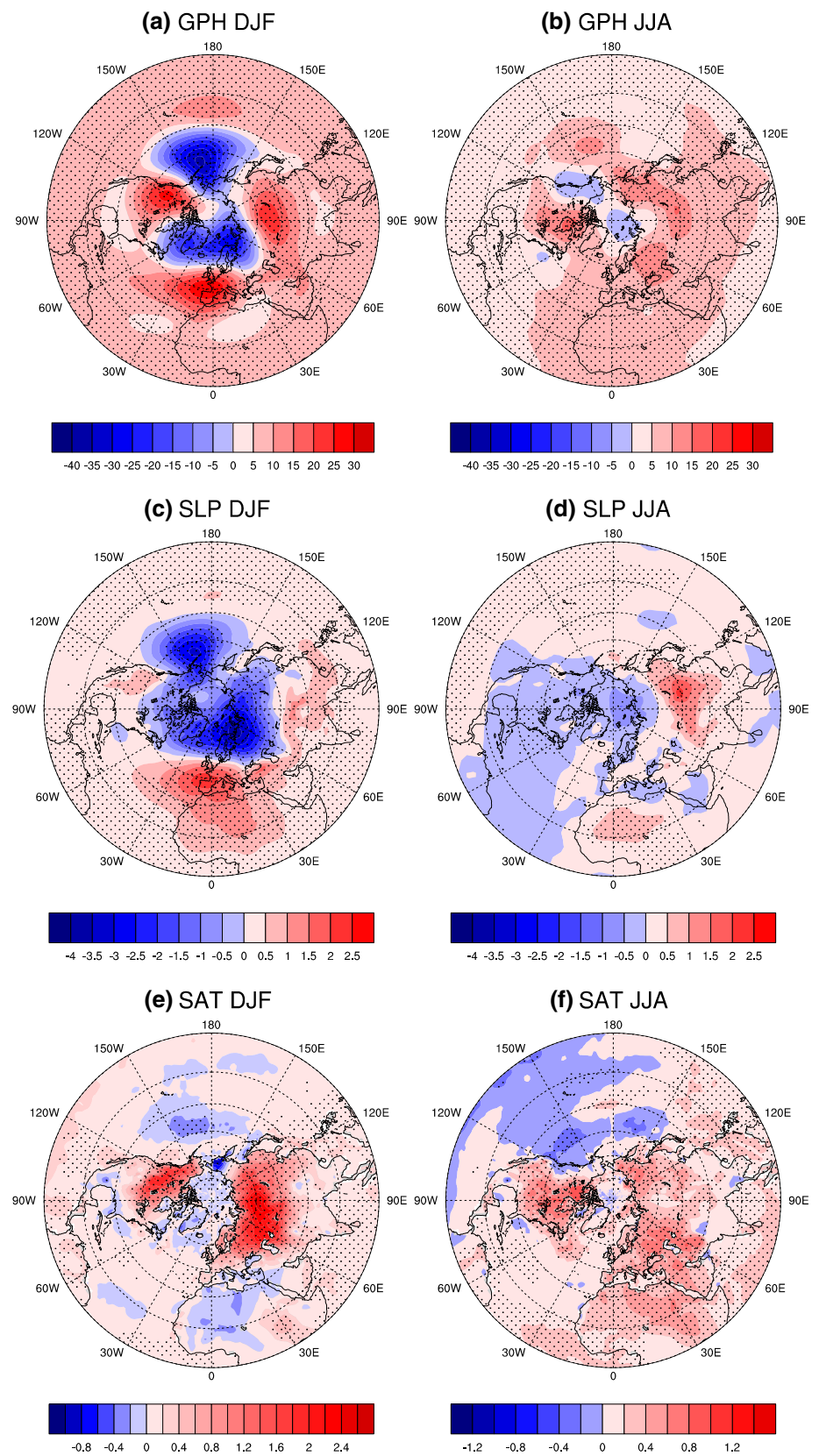
accelerate winter warming progress under global warming. But the COWL pattern is not very obvious in summer GPH, SLP or SAT regression field, which is why we define summer LSI by averaged SAT in land and ocean, rather than four centers of the COWL pattern as same as He et al. (2014). Consistent with the result from JRA-55 dataset (Fig. S5), in summer, the areas of negative anomalies in the Arctic is smaller than that in winter and the GPH regression pattern is characterized by a seesaw between middle and high latitudes, especially in the Eurasian, where the gradient of SLP is significantly stronger. The responses of GPH and SLP to summer LSI changes indicate that the role of zonal asymmetric thermal forcing might be different in summer with in winter. The similar result can also be seen in the regression pattern on the interannual and decadal variability of the winter summer LSI.

4.2 Zonal mean westerly wind and AO

Planetary waves are forced in the troposphere by orography and patterns of diabatic heating associated with the land-sea distribution (Andrews et al. 1987) and play an important role in bridging the surface temperature changes and internal variability of atmospheric circulation. The land-sea thermal forcing is an important external forcing for planetary waves. Chen et al. (2005) pointed out that the amplitudes of the planetary waves in the lower troposphere over middle and high latitudes is affected by the impact of the westerly wind intensity on the vertical propagation of planetary waves. He et al. (2014) demonstrated that during the winter with positive LSI index, the intensified westerly provides an unfavor environment to the formation of blocking. Although the planetary waves in summer is much weaker than winter, it is interesting to investigate whether the spatial pattern of thermal forcing is related to the propagation of planetary waves and further influence the zonal westerly changes.

To investigate this relationship, we compare the correlation between AO and LSI in winter and summer (Fig. 4). The AO index in Fig. 4 is used to measure the intensity of the mid- to high-latitude westerly wind. Li and Wang (2003) defined a modified AO index by the difference in zonal mean SLP between 35°N and 65°N from the monthly
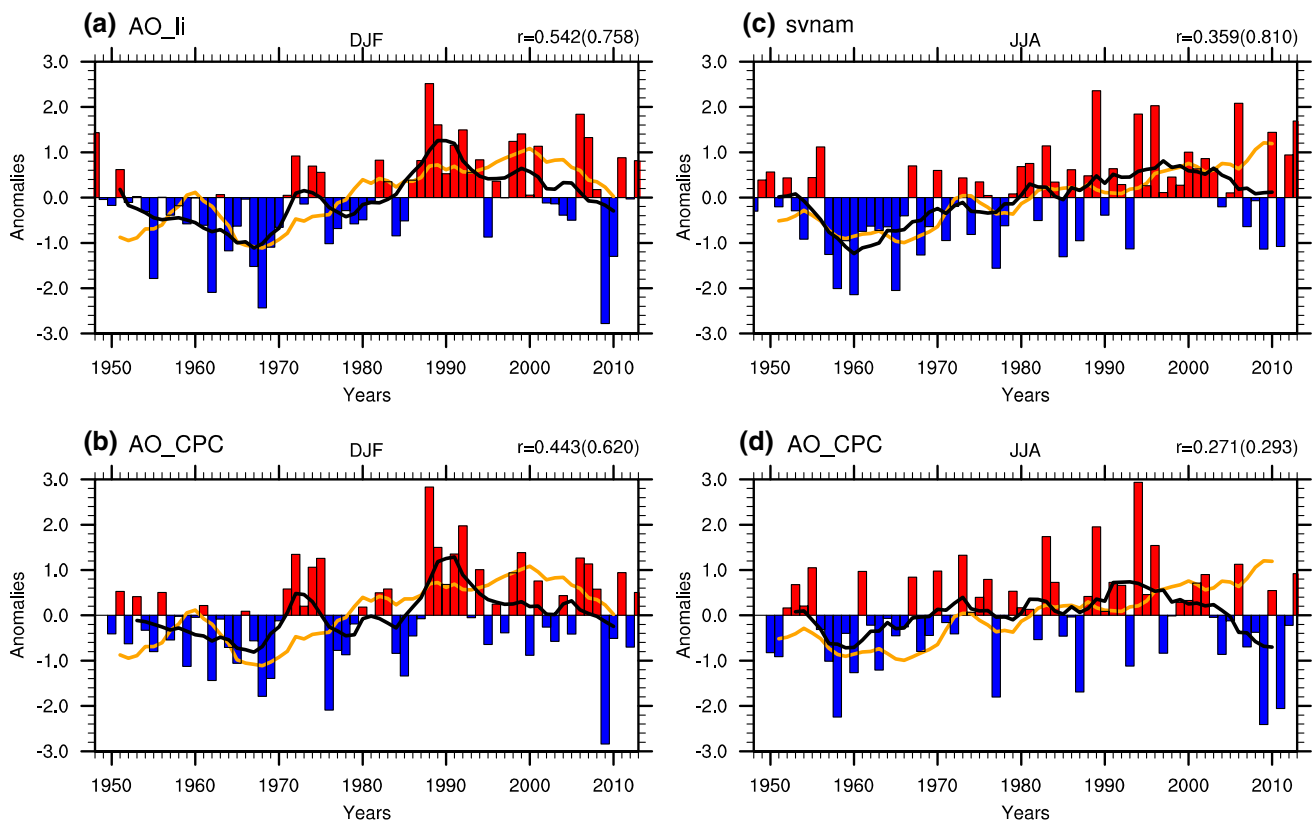

Fig. 4 Left panels Winter (DJF) mean time series of the AO index defined by Li (**a**) and CPC (**b**) during 1948–2013. The black curves indicate 7-year Gaussian-type filtered values. The yellow curves indicate 7-year Gaussian-type filtered winter LSI values. The right corner labels are the correlation coefficients between weighted AO index and weighted LSI index, the brackets are the correlation coefficients through gauss-type filter. Right Panels same as the left panels, except for the summer SVNAM index (**c**) and the summer AO index from CPC (**d**) during 1948–2014

NCEP reanalysis data. They pointed out that the modified AO index contains a larger signal-to-noise ratio than the traditional zonal index. The traditional AO index in Fig. 4b is defined by the leading EOF of monthly GPH and downloads from Climate Prediction Center (CPC). In winter, the correlation coefficients between the LSI and the AO index from Li and CPC were 0.75 and 0.62, respectively, after applying a 7-year Gaussian filter. All coefficients significantly exceed the 99% confidence level. However, traditional AO index including modified AO index reveals a seesaw of atmospheric mass between middle and high latitudes, which is a winter-dominant mode because atmospheric variability is largest in winter. Ogi et al. (2004, 2005) performed an EOF analysis for each individual calendar month to distinguish the seasonal variations of the Northern Hemisphere annular mode (NAM). They demonstrated that summer NAM has a smaller meridional scale and the conventional AO index does not correctly extract the summer dominant mode. Consistent with previous studies, Fig. 4 shows the correlation coefficient between conventional summer AO index from CPC and summer LSI is 0.29, which is much less than that between seasonal varied NAM and summer LSI (0.81). The result implies that there is a close relationship between summer annular mode and land-sea thermal contrast, which is not reflected by conventional AO index.

Figure 5 shows the cross sections of zonal-mean westerly regressed onto the winter and summer LSIs during 1948–2013. Shading indicates regression coefficients exceed the 90, 95, 99% confidence level, respectively. Consistent with the result from JRA-55 (Fig. S6), Fig. 5a shows that increased winter LSI corresponds to the clearly enhanced westerly wind appeared around 60°N, which results in a

poleward shift of subtropical jet stream. During winters within positive phase of LSI, the upward waves propagation from the troposphere into the stratosphere become weaker and the low-latitude waveguide prevails, which means that the forcing exerted by planetary wave activity on the westerly wind is weaker due to deceased land-sea thermal contrast. However, the structure of zonal-mean westerly wind regressed onto summer LSI shows a similar structure with winter, but the positive westerly changes in summer is more north shift than winter. In winter, enhanced westerly in middle and high latitude could decrease the blocking event numbers, which is consistent with observations. However, in summer, the enhanced westerly in high latitude strengthens the polar jet and in general, strong westerly does not favor the blocking events, which is contradict with observational increased summer blocking. The mechanism between summer blocking and LSI or enhanced westerly will be explained in detail in Sect. 6.

5 The opposite effect of LSI on winter and summer blocking

The prominent features of the midlatitude low-frequency atmospheric variability are characterized by two possible dynamic equilibria (wave-like flow or zonal flow). Blocking is the breakdown of the high kinetic energy state of atmosphere and take into a low kinetic energy level state, which exhibits a significant meridional component. During winters, blocking can induce extremely cold weather, while during summers, blocking is often associated to severe droughts and heat waves
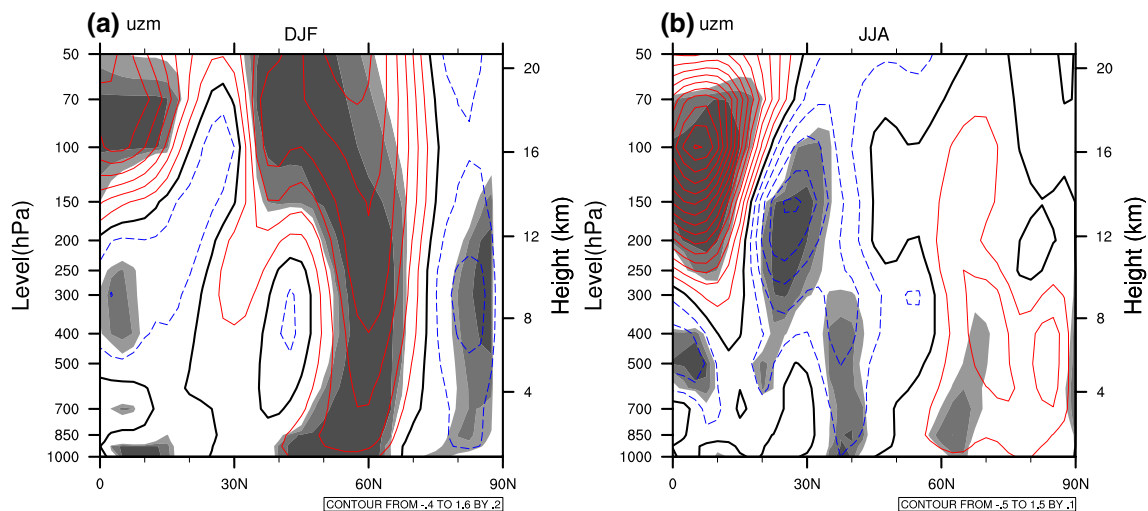

Fig. 5 Latitude-height cross sections of the zonal mean zonal wind regressed on the winter LSI (**a**) and the summer LSI (**b**). the counter interval of Fig. 4a is 0.2 m/s and the counter interval of Fig. 4b is 0.1 m/s. Red solid contours denote positive values, and blue dashed contours denote negative values, zero counter is drawn by thick black line. The shading areas indicate regression coefficients exceed the 90, 95 and 99% confidence level, respectively

(Shabbar et al. 2001; Tyrlis and Hoskins 2008; Tachibana et al. 2010; Luo et al. 2014a, b).

Here, an objective blocking index defined by Tibaldi and Molteni (TM, 1990) is used in this study. Because blocking events are relatively more frequent over the central Pacific Ocean and the eastern North Atlantic Ocean, and relatively less over the continents, four blocking sectors as shown in Table 1 are defined to determine sector blocking events. A given longitude is defined as blocked on a specific day if southern GPH gradient is larger than 0 and northern GPH gradient is less than -10 m/degree. If a blocking-like pattern exists over three or more adjacent longitudes and last for 5 days or longer, it is considered a regional blocking event. The blocking days are obtained by simply counting the number of days considered as blocked by blocking index during winter or summer. The blocking days in NH is the sum of blocking days in four sectors. The details of blocking determination method can be found in references (He et al. 2014).

To investigate the response of blocking days to LSI in winter and summer, a composite analysis is carried out to measure the impact of land-sea thermal contrast on the blocking. In this study, we select the positive and negative LSI cases in winter and summer when the absolute normalized value of the LSI is larger than 1.0. Based on this criterion, the years in the positive and negative phase of LSI in winter and summer are shown in the Table 2. The parameters of blocking, such as the mean blocking days per winter or summer, duration and event numbers, are shown in Table 3. To get the robust conclusion, we make the same composite analysis for the JRA-55 dataset (Table S1 and S2) and get the similar result. To examine the sensitivity of result to the positive and negative years for composite analysis, we repeat the composite analysis for the positive and negative LSI cases when the absolute normalized value of the LSI is larger than 0.5 and get the consistent result (Table S3 and S4). The result shows that the winter blocking is decreasing with increased winter LSI, and the summer blocking is increasing with increased summer LSI, with linear trends of -0.159 and 0.065 day/year, respectively, without the 90% confidence level. The differences of the trends of blocking days in winter and summer might be related to the weak increase of summer LSI. The mean blocking days in winter during negative LSI phase was 35 days longer than that during the positive LSI phase, and the mean blocking days in negative summer LSI phase is nearly equal to (slightly more than) that in positive summer LSI phase based on the NCEP (JRA-55) dataset. To further analyze the changes of duration and event

Table 1 Blocking sectors defined in this study

	Euro-Atlantic		Pacific	
Sector	ATL	EUR	WPA	EPA
Domain	(100°W, 0°)	(0°, 90°E)	(90°E, 180°)	(180°, 100°W)

Table 2 The year in the positive phase and negative phase of LSI in winter and summer

	Positive	Negative
Winter	1980, 1982, 1988, 1991, 1994, 1998, 1999, 2001, 2003, 2006	1949, 1950, 1953, 1955, 1956, 1966, 1968, 1971, 1978, 1984
Summer	1988, 1995, 1998, 2001, 2002, 2006, 2007, 2010, 2011, 2012	1950, 1951, 1956, 1957, 1958, 1965, 1967, 1968, 1978, 1992

number, the distributions of blocking frequency in winter and summer are investigated as shown in Fig. 6. In winter, the average duration of blocking event was 9.69 and 11.44 days during the positive and negative phase, respectively. Because most of the blocking events (~75%) in the whole NH are less then 10 days, to classify short and long duration blocking, we categorize blocking event as short-lived blocking event with duration is 5–9 days and long-lived blocking event with duration is longer than 10 days (Dunn-Sigouin and Son 2013). By comparing the durations and event numbers of short-lived and long-lived blocking events, the decrease of mean blocking days during positive phase is found to be caused by the fewer long-lived blocking events, e.g. 35 events in positive phase and 52 events in negative phase. This result is consistent with He et al. (2014). In summer, the average duration of blocking in positive phase (9.07 days) was less than that (10.37 days) in negative phase, which is mainly caused by the decrease of the duration of long-lived blocking from 16.11 (negative) to 13.58 (positive). At the same time, total event number of the

Table 3 Composite analysis of blocking parameters (rows) for the Northern Hemisphere in winter and summer (columns)

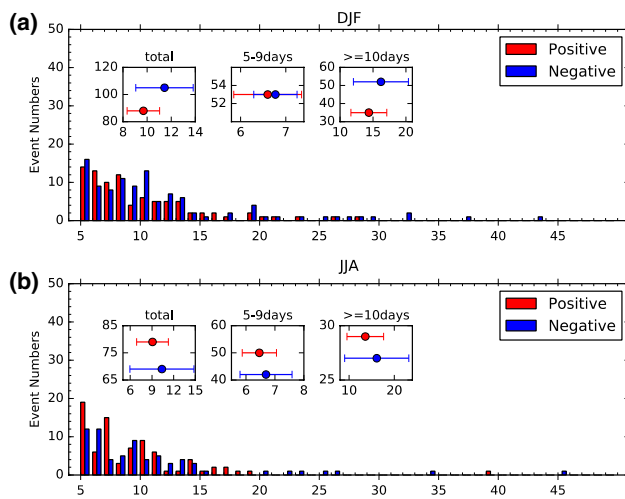|			Winter	Summer
Trend (day/year)			-0.159	0.065
Mean days		Pos	85.3	71.7
		Neg	120.2	71.6
Duration (days)	Total	Pos	9.69	9.07
		Neg	11.44	10.37
	Short	Pos	6.60	6.46
		Neg	6.77	6.69
	Long	Pos	14.37	13.58
		Neg	16.21	16.11
Event number	Total	Pos	88	79
		Neg	105	69
	Short	Pos	53	50
		Neg	53	42
	Long	Pos	35	29
		Neg	52	27

Fig. 6 The distributions of Northern Hemisphere blocking event durations in winter (**a**) and summer (**b**) for positive LSI phase and negative LSI phase. The attached panels are the composites of the sum of blocking events include total, short period (5–9 days) and long period (≥ 10 days) and the corresponding mean durations for positive and negative LSI phase

Fig. 7 Changes in land-sea contrast and blocking days in winter (**a**) and summer (**b**) during 1948–2013. The red dots indicate the values during 1948–1980, the blue dots indicate the values during 1981–2013. The black lines indicate the regression lines. The values in the right corner are the sensitivities of blocking days to LSI, the star indicates the significant values at the 99% confidence level

summer blocking increases from 60 (negative) to 79 (positive). The short-lived blocking events more frequently occur with equal durations, but long-lived blocking events significantly increase in numbers, with decreased durations. For example, JRA-55 dataset suggests that the long-lived blocking frequency increased from 1.5 per year (negative) to 2.6 per year (positive) as shown in the Table S2. However, the duration of total blocking events in ATL and EUR show a consistent variation in winter and an opposite variation in summer, which maybe contribute to the weak increase of summer blocking days (not shown). Because the response of regional blocking makes the aim of this paper complex, so we will further investigate the response of regional blocking to LSI changes in next paper.

These results show that the opposite effect of increased LSI on winter and summer blocking and induce opposite trends. However, the ways inducing the changes of winter and summer blocking days are different. The winter long blocking decreases both in blocking number and duration, but the summer long blocking increases in the event numbers and decreases in the duration. Consistent with Kamae et al. (2014b), the summer LSI increases due to the increased CO_2 concentration, and amplifies the resonance of planetary waves induced by thermal and topographic forcing by following the Charne-DeVore's mechanism (Zhu et al. 1982). The increased summer LSI and blocking form a positive feedback, named LSI-blocking positive feedback, which is contradict with the decrease of blocking duration, especially for long blocking. However, different with winter feedback, the convergence of EP flux induced by summer LSI has a poleward shift compared to winter scenario and generates a
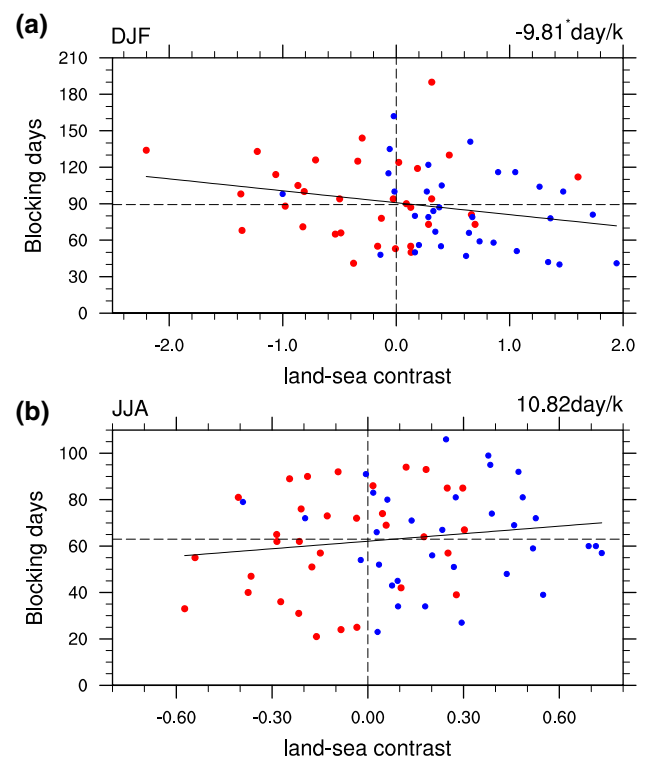
double-jet structure, which can provide an environment to favor the formation and maintenance of blocking and form a positive feedback (named LSI-double-jets-blocking positive feedback) based on Petoukhov's theory. Therefore, the significant decrease of duration of long blocking in summer is caused by another mechanism (discussed in Sect. 6), and the increase of event numbers in both short and long blocking is caused by LSI-blocking and LSI-double-jet-blocking positive feedback. Because the opposite effect of different feedbacks on the changes of summer blocking, the summer mean blocking days have a weak increase.

To investigate the link between asymmetric warming and blocking changes, we compare the sensitivity of blocking to LSI in winter and summer as shown in Fig. 7 (NCEP) and Fig. S7 (JRA-55). Here, we use the ratio of blocking days and LSI indicating the sensitivity of blocking to LSI. The sensitivity of blocking in winter is − 9.81 day/K with 90% confidence level of student's t test, which is similar to the absolute value in summer (10.82 day/K without 90% confidence level of student's t test). We also use bootstrap method to examine the significance of regression coefficients, the mean value of winter sensitivity of blocking with

1000 resamples is − 9.39 day/K (the corresponding standard deviation is 4.16 day/K) and that in summer is 9.66 day/K (the corresponding standard deviation is 7.46 day/K). The result implies the slower warming in summer associated with increased summer blocking may be caused by the weaken increase of summer LSI, rather than the sensitivity of blocking. The further analysis of blocking sensitivity will be discussed in Sect. 7.

6 The physical mechanism

6.1 The role of transient and stationary wave for double-jet

Ogi et al. (2005) analyzed the 2003 Europe blocking and demonstrated that the double-jet structure of zonal wind has an important impact for extending strong subtropical high from Africa toward northeast Europe. But the mechanism associated with blocking and double-jet is not clear although the QRA theory provides an insight in understanding the link between them. According to Eq. 2 in Petoukhov et al. (2013), between double jet centers, the reduced westerlies and narrow flow tunnel may lead to more frequent appearance of the northern turning points of l^2 (meridional wave number, l) for the free waves with k = 6–8, which means more blocking happen probability. However, whether the relationship between double jets and summer blockings follows Petoukhov's theory need further investigation using observational data. Rikus (2015) developed an algorithm to determine double jets. This allows us to calculate double jets. First, a local maximum and minimum filter is applied to the zonal-mean U field by a 25-point maximum/minimum stencil leading to a zonal-mean U field U_{Min} and U_{Max}. Then Rikus' algorithm examine for each grid cell whether $U_{Max}(xy)$–$U_{Min}(xy) > 0.4$ and whether $U_{Max}(x, y) = U(xy)$. Only points where both conditions are fulfilled are considered as zonal-mean jet stream cores. Fig. S8e shows the days with double jets calculated by Rikus' algorithm in red. The frequency of double jets may be overestimated because the jet streams are so wavy and hence the algorithm find two maximum cores instead of one. As suggested by Molnos et al. (2017), the jet stream can merge in some regions and separate in other regions. Obviously, Rikus' algorithm does not consider this situation and overestimate the frequency of double jets. However, the result could help us to understand the casual relationship between double jets and blockings. Fig. S8a-d show the summer blocking days during 1948–2015 in four sectors. We analyse statistically whether the double jets occur on the day before blocking, as shown in the Fig. S8f. The results suggest that the double jets have occurred on the day (1 day earlier than the blocking) at a probability of 67.8%, even reach to 83.5 when consider the

formation of double jets is a little late, occurring on the first day of the blocking. Therefore, the double jets is not caused by the blocking through separating the westerly wind. Although Petoukhov's theory can not describes the formation and decay of blocking, it gives an insight into the link between the double jets and blockings. Further investigation is needed, but is beyond the scope of the present study.

It's worth noting that the role of transient and stationary wave in the formation of double-jet. Figure 8 (NCEP) and Fig. S9 (JRA-55)_show the zonal mean poleward eddy momentum flux, $u'v'$, regressed with the LSI index. Fig. S9 shows the zonal mean of the gradient of the poleward eddy momentum flux, $-\frac{\partial \overline{u'v'}}{\partial y}$, regressed with the LSI index. The primes indicate deviation from the zonal mean, and overbars indicate zonal average. Total eddy momentum flux is calculated from daily mean data and stationary eddy momentum is calculated from monthly mean data, the transient eddy momentum flux is calculated by subtracting the stationary flux from the total eddy momentum flux. Consistent with previous study, total eddy flux in winter is mainly attributed to stationary waves because transient waves are very weak, but transient waves in summer is equally or even more important than stationary waves to maintain the wave forcing. Comparing the positions of the stationary waves forcing and the transient waves forcing regressed on summer LSI (Fig. 8d–f, Fig. S9d-f and Fig. S10d-f), it is clear that the double-jet structure is mainly caused by stationary waves because of the matching locations, although it is weaker than transient waves. Ogi et al. (2005) suggested that the transient waves forcing regressed on summer NAM index contribute more than stationary waves forcing to the double jet structure surrounding the Arctic Ocean. It need mention that Ogi et al. (2005) gets this conclusion by regression field, which only demonstrates that the influence of summer NAM on polar jet depends more on transient waves forcing. Figure 8d-f and Fig. S9d-f demonstrate that the influence of summer LSI on polar jet depends more on stationary waves forcing. The positive westerly anomalies induced by stationary waves forcing are matching the locations of double jets and the transient waves forcing mainly occur around 60°N, where is between the double jets (Fig. S10e-f). However, stationary waves are generally generated by zonal asymmetric thermal forcing associated with land-sea distribution, which induces westerly changes by EP flux converge and transient waves forcing are generally considered to associate with baroclinicity induced by meridional thermal contrast, which induces westerly changes by thermal wind relationship. Here, we propose a mechanism to explain the role of summer NAM and summer LSI in asymmetric warming progress (Fig. 9). During the recent decades, sea ice rapidly declines and decreases the meridional temperature gradient, which induces a negative AO-type circulation (Wu et al.
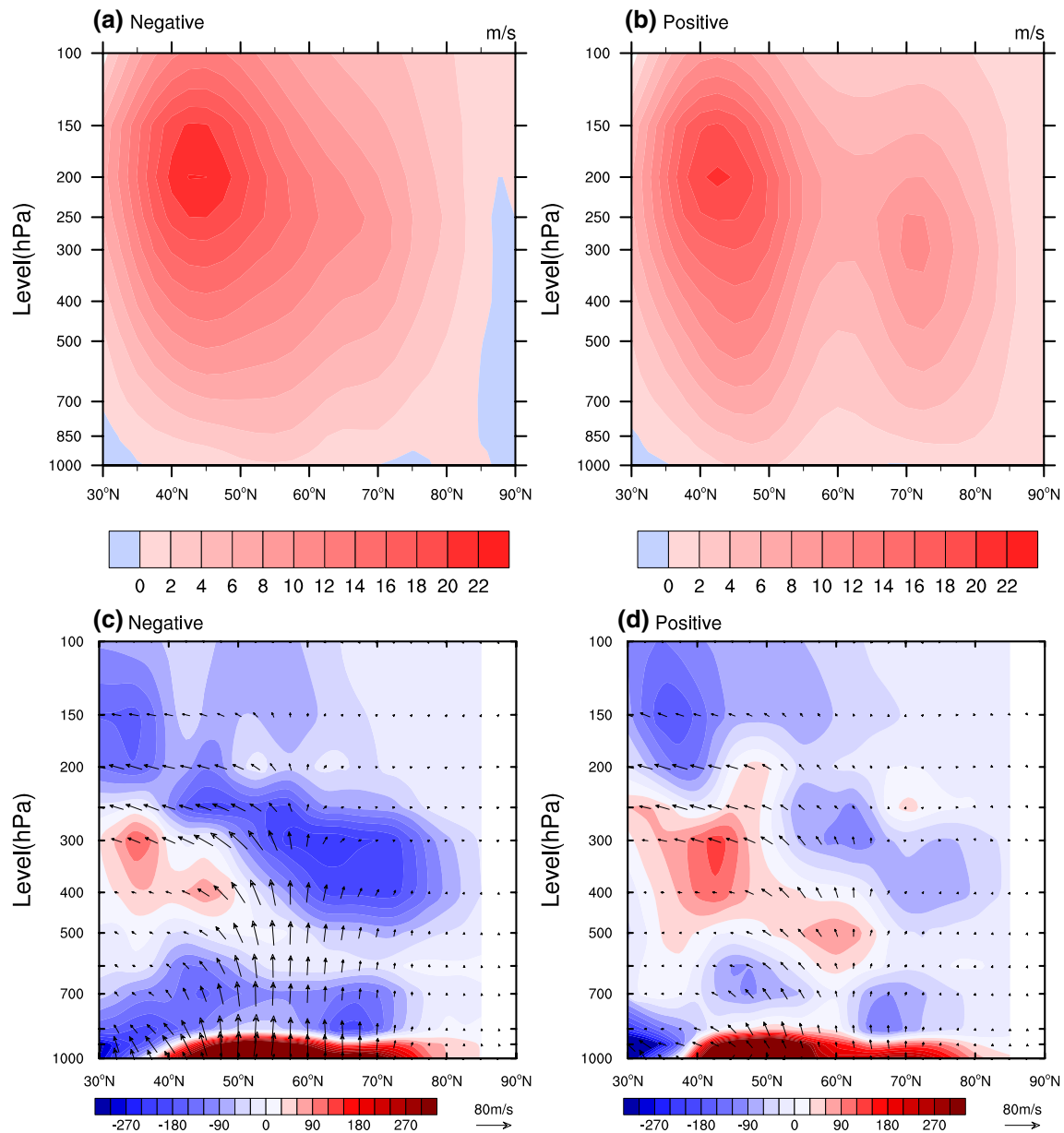
Fig. 8 Top panels the latitude-height cross sections of zonal-mean zonal wind for negative daily LSI (**a**) and positive daily LSI (**b**). contour intervals are 2 m/s. Bottom panels same as the top panels, except for Eliassen-Palm flux and its divergence. The reference arrow for the EP flux vector of 80 m²/s² is shown at the bottom. The contour intervals of EP flux divergence are 30 m/s². The vertical length of the arrow is scaled by pressure

2016). This result suggests that weaken westerly around Arctic Ocean does not support the appearance of double-jet structure. Following Petoukhov's theory, without the help of double-jet structure, the blocking frequency should decrease, which contradicts with observations. Therefore, the increase of the observational blocking associated with summer extremes are caused by summer LSI, rather than summer NAM. And sea ice loss can induce a negative AO-type circulation with significant summer surface cooling trend over

midlatitude, which reduces the warming (Wu et al. 2016). Therefore, the summer LSI has a lower trend relative to winter and induces less summer blocking response.

However, Summer NAM index are defined by the meridional structure to measure the degree of seesaw phenomenon between midlatitude and high latitude. Therefore, when double-jet occur induced by extreme high LSI, the summer NAM must be high index, which is consistent with high correlation between summer NAM and LSI. Therefore, during

Fig. 9 The schematic diagram of winter and summer feedback, the blue solid lines indicate the winter positive feedback between the LSI and blocking, the green solid (dotted) lines indicate the summer positive (negative) LSI-blocking feedback, the orange lines indicate the changes of asymmetric warming in the past, present and future time. The red and black dash lines indicate the factors may influence the summer LSI-blocking feedback, but the mechanism need further investigation

recent decades, the double jets are maintained by stationary waves forcing associated with zonal asymmetric thermal forcing.

Because the percent of summer blocking days in the sum days during summer was much less, monthly averaged result might contain too much noise and does not clearly show the composite differences. Therefore, daily summer LSI is used in the composite analysis. We choose the positive cases when the daily summer LSI is larger than 3.0 and choose the negative cases when the daily summer LSI is less than −2.782, in order to have equal sample days (43 days). We also make the composite for more sample days in phases (up to 1120 days), the results are similar. Here, the daily summer LSI with extreme high or low index days is shown in Fig. S11. Figure 8 (NCEP) and Fig. S12 (JRA-55) show the cross section of zonal mean westerly and Eliassen-Palm (EP) flux by daily composite analysis. In both positive and negative phase of summer LSI, the EP flux is convergent in the middle troposphere over high latitude, resulting in an easterly wind forcing on the westerly wind. In negative phase of summer LSI, the high latitude polar jet disappears due to the stronger EP flux convergence, which exerts a strong easterly wind forcing (Fig. 8a, c and Fig. S12a, S12c). Opposite scenario occurs in positive phase of summer LSI, so polar jet appears due to weaker convergence of EP flux (Fig. 8b, d and Fig. S12b, S12d). Although the double-jet structure is important for the blockings magnified by quasiresonance amplification mechanism, the present analysis shows it only

exist during summer LSI is very high. Therefore, the summer LSI-double-jets-blocking positive feedback is limited, which maybe induce the slower summer warming than winter.

Another important question is the mechanism explaining the decrease of duration of summer blockings. As shown in Fig. 5b, the westerly wind around 60°N regressed on the LSI does not have significant change, which is consistent with the Fig. S10, because the stationary waves forcing and the transient waves forcing have the opposite effect on the westerly wind. However, the transient waves forcing induced by the LSI increase become stronger around the 60°N. As suggested by Luo (2017a, b), the duration of blocking depend strongly on the strength and vertical shear (VS) of the mean westerly wind (MWW). Under strong MWW and VS conditions, synoptic-scale eddies are stronger and the growth of blocking is rapid, the resulting blocking is less persistent with large amplitude and has a marked retrogression. Here, when summer LSI is very high, the westerly wind between double jets does not significantly decrease or increase, but the transient waves activities induced by increasing summer LSI become stronger (Fig. 10f and Fig. S10f). Following Luo's theory, the strong synoptic-scale eddies induce large amplitude of blocking, which corresponds to the rapid retrogression and less duration. Therefore, the higher summer LSI makes the duration of blocking decrease through
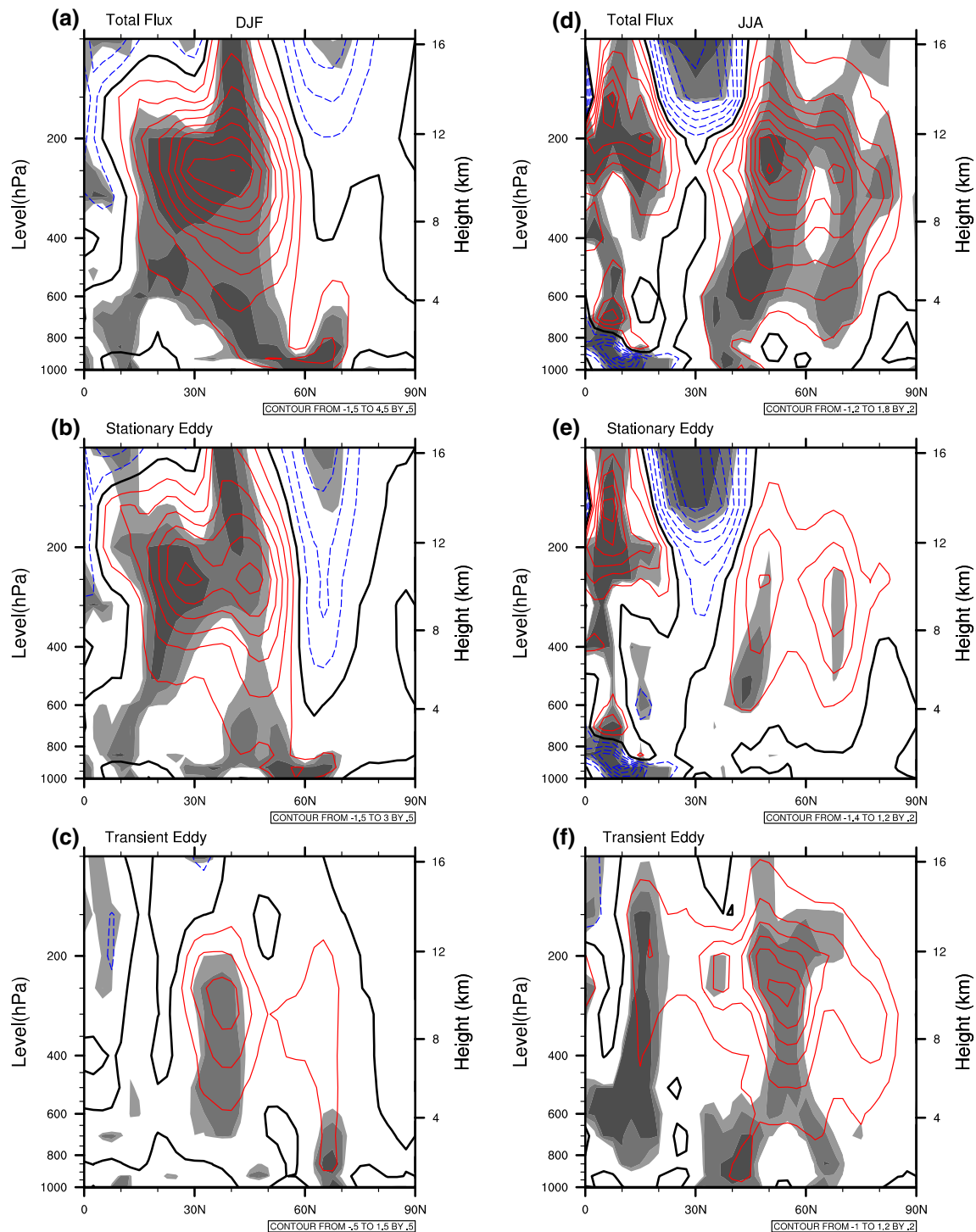
Fig. 10 Winter (**a**–**c**) and summer (**d**–**f**) poleward eddy momentum flux regressed on the winter LSI and summer LSI. (top) Total eddy momentum flux. (middle) Stationary eddy momentum flux. (bottom) Transient eddy momentum flux. The contour interval is 0.5 m^2/s^2 in winter, 0.2 m^2/s^2 in summer. Red solid contours denote positive values, and blue dashed contours denote negative values, zero counter is drawn by thick black line. The shading indicated regression coefficients exceed the 90, 95 and 99% confidence level, respectively

Table 4 a list of CMIP5 GCMs used in this study with a brief description. The historical and RCPs run from each model are used. The first ensemble run is used if a model has multiple ensemble runs

	Model name	Rosolution (lon by lat)	Origin
1	ACCESS1-0	1.875×1.25	Commonwealth Scientific and Industrial Research Organization, Australia
2	ACCESS1-3	1.875×1.25	Commonwealth Scientific and Industrial Research Organization, Australia
3	CanESM2	2.815×2.815	Canadian Center for Climate, Canada
4	CMCC-CM	0.75×0.75	Centro Euro-Mediterraneo per I Cambiamenti, Italy
5	CMCC-CMS	1.875×1.875	Centro Euro-Mediterraneo per I Cambiamenti, Italy
6	CNRM5-CM5	1.40×1.40	Centre National de Recherches Meteorologiques, France
7	GFDL-CM3	2.5×2.0	Geophysical Fluid Dynamics Laboratory, USA
8	GFDL-ESM2G	2.5×2.0	Geophysical Fluid Dynamics Laboratory, USA
9	GFDL-ESM2M	2.5×2.0	Geophysical Fluid Dynamics Laboratory, USA
10	IPSL-CM5A-LR	3.75×1.875	Institut Pierre-Simon Laplace, France
11	IPSL-CM5A-MR	2.5×1.25	Institut Pierre-Simon Laplace, France
12	IPSL-CM5B-LR	3.75×1.875	Institut Pierre-Simon Laplace, France
13	MIROC5	1.40×1.40	Atmosphere and Ocean Research Institute, Japan
14	MIROC-ESM	2.815×2.815	Atmosphere and Ocean Research Institute, Japan
15	MIROC-ESM-CHEM	2.815×2.815	Atmosphere and Ocean Research Institute, Japan
16	MPI-ESM-MR	1.875×1.875	Max Planck Institute for Meteorology, Germany
17	MPI-ESM-LR	1.875×1.875	Max Planck Institute for Meteorology, Germany
18	MRI-CGCM3	1.125×1.125	Meteorological Research Institute, Japan
19	NorESM1-M	2.5×1.875	Norwegian Climate Centre, Norway

induced more transient waves activities, which forms a negative feedback, named "LSI-transient-waves-blocking" negative feedback.

6.2 The simulated response of blocking to land-sea contrast change

To verify the feedback between summer blocking and LSI, we use the outputs from 19 global climate models (Table 4) to undertake a sensitivity analysis. To facilitate the calculation of blocking by TM criteria, all model simulations are firstly interpolated to the same resolution (2.5° × 2.5°). The simulations are obtained from the CMIP5 multi-model data archive (https://pcmdi.llnl.gov/search/esgf-llnl/). Historical and future scenarios (RCP4.5 and RCP8.5) simulations are selected to examine the response of blocking to the land-sea thermal contrast change in this study. The projected climatology of the last 30 years (2071–2100) is used to compare with the historical climatology (1976–2005). The boundary conditions for each experiment are described in Taylor et al. (2012).

Figure 11 shows the time series of the winter and summer LSI in the historical, RCP4.5 and RCP8.5 experiments. In historical run, the LSI gradually increases under global warming and the change of LSI in winter is much more than that in summer, which is consistent with observation. In projected scenarios, the LSI in winter and summer both increases faster than historical run due to the increasing

CO_2 concentration, which is consistent with previous study (Kamae et al. 2014a, b). Comparing the winter LSI between historical and projected runs, the winter LSI in the RCP8.5 is near 1.2 °C higher than that in historical run, which is much larger than that in summer (~ 0.3 °C). The result suggests the feedback in winter is stronger than that in summer, when facing the same greenhouse forcing.

To verify the different sensitivity of winter and summer feedback responding to same forcing, we investigate the sensitivity of blocking to the changes of LSI in winter and summer from every individual model simulations as shown in Fig. 12. Under RCP4.5, all models, except for ACCESS1-3 and CNRM-CM5, show a decreased averaged blocking days and an increased LSI in winter, although there are very large standard deviations between models. However, all models, except for ACCESS1-3, GFDL-ESM2M, IPSL-CM5B-LR and MIROC-ESM, show an increased summer LSI and they are less than that in winter by different degrees. But the summer blocking days show the different response in the RCP4.5 experiment relative to historical experiment. Only CNRM-CM5, IPSL-CM5A-LR and MIROC-ESM-CHEM model simulate the increasing blocking days in summer. Most of other models show a decreasing trend of blocking days, when CO_2 concentration increases, which may be partially caused by the capability of model to simulate blocking. Masato et al. (2013) also found summer blocking decrease in general when investigating the changes of summer blocking in the twenty-first century. Much of the blocking errors
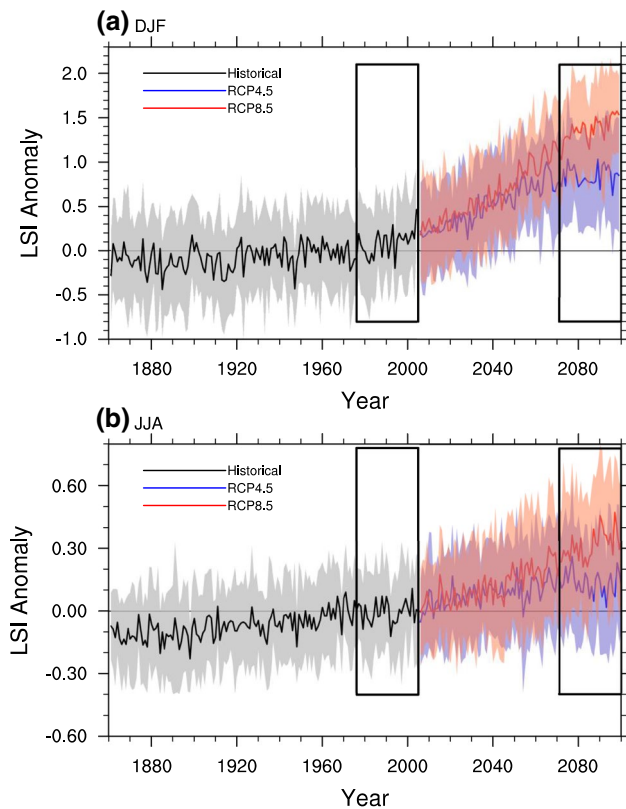
Fig. 11 Time series of the winter LSI (**a**) and the summer LSI (**b**) in the 1pctco2 and picontrol experiments. The red solid curve represents the ensembles mean of the 1pctco2 experiment, and the blue dashed curve represents the ensembles mean of the picontrol experiment. The shading denotes one standard deviation of the seven models from the picontrol/1pctco2 simulations. The boxes indicate the last 20 years to compare blocking day changes

blocking to LSI is higher than that in summer due to the limits of summer feedback mechanism.

7 Discussion and conclusion

Although the above analysis demonstrates that there is a statistic relationship between summer blocking and summer LSI, we need to provide a physical mechanism to explain the statistic relationship and verify the mechanism. Here, we provide a positive feedback between summer blocking, summer LSI and double-jet structure as shown in Fig. 9. When CO_2 concentration increases due to human activity, the land in summer is gradually more warming than ocean, the summer LSI starts to increase. The increasing land-sea thermal contrast, as an external forcing, could induce the positive anomaly of zonal westerly at high latitude (north of 60°N) by adjusting the EP flux convergence caused by planetary waves activity. When summer LSI exhibits a high index, the double jet structure appears. Previous studies (Grise and Polvani 2014; Kawatani et al. 2012) suggested that the direct radiative forcing of CO_2 drives a poleward jet shift, which may help the double-jet structure more narrow. Following Petoukhov's theory, the tunnel between two jet centers provides a narrow and reduces westerly environment, which may lead to more frequent appearance of the northern tuning point for the free waves with k = 6–8 (Petoukhov et al. 2013, 2016). In addition to the increase of blocking frequency, the amplitudes of summer blockings could be magnified through the quasiresonance after trapping midlatitude waveguides of free synoptic waves with k = 6–8. The more heat waves in summer could further increase the land-sea thermal contrast by more warming in land. Therefore, summer blocking, summer LSI and double-jet structure form a positive feedback to accelerate the warming in summer. In this feedback, there are two questions still need to be clearly answered. One question is whether is the double-jet structure caused by summer LSI because Ogi et al. (2005) pointed out that summer NAM is also related to double-jet structure. Another question is that why the intensity of summer positive feedback is weaker than winter positive feedback and how to explain the seasonal asymmetric warming.

In this study, we investigate the opposite impact of the land-sea thermal contrast changes on blocking in winter and summer, and provide a mechanism to explain the link between the response of blocking to LSI and the asymmetric warming in season scale. Associated with seasonal asymmetric warming, the trend of winter LSI was near six times the trend of summer LSI. Regression analysis determines that when the summer LSI is higher, the strong EP flux convergence becomes weaker and induces polar jet appearing in the high latitude. Following Petoukhov's quasiresonant amplification mechanism of planetary waves, the double-jet
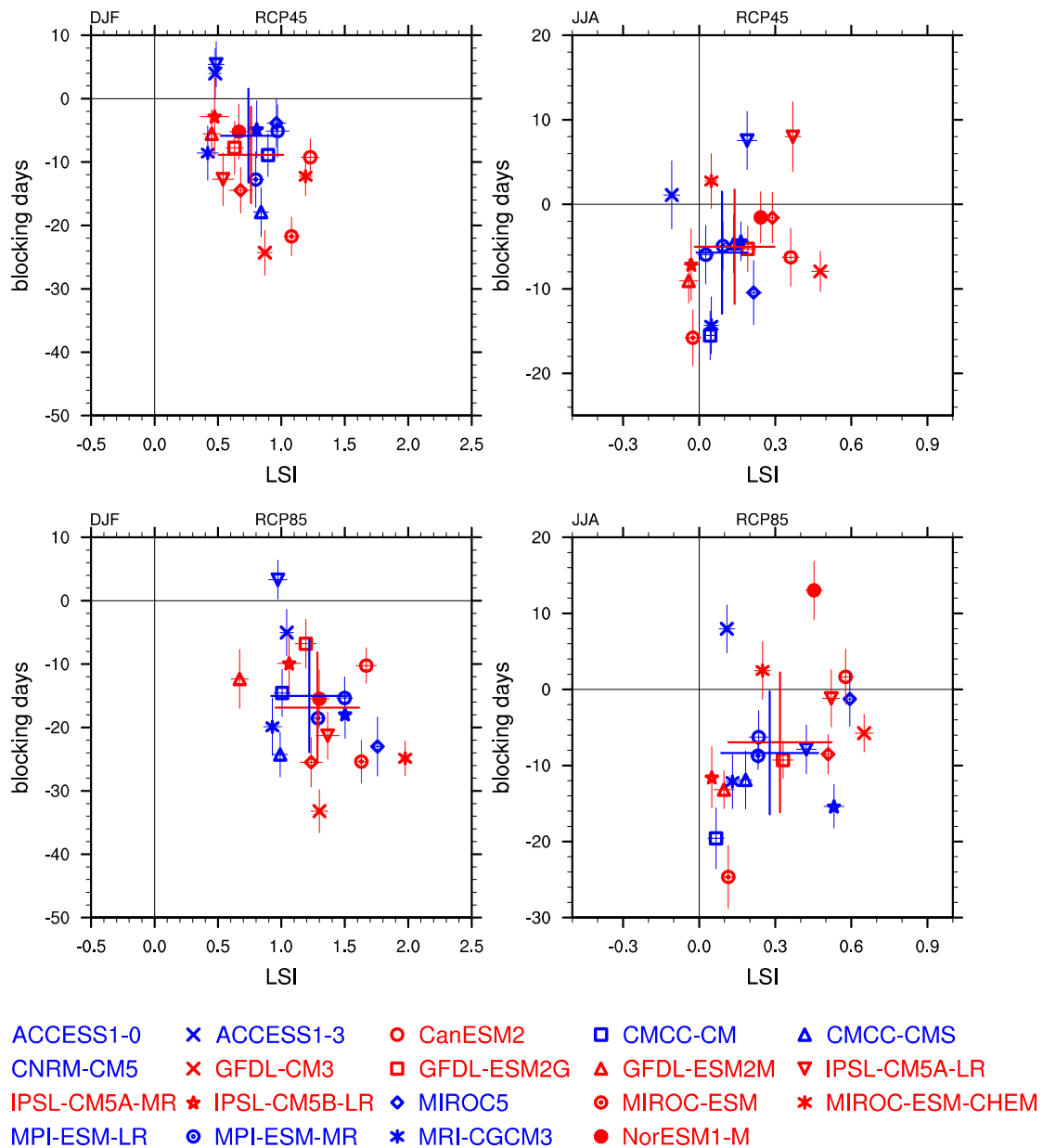
can be directly attributable to the climatological biases and low horizontal resolutions of the model (Scaife et al. 2010). However, the mean values of the nine high-resolution ($<2°$) models (blue markers) also simulate the decreased summer blockings, which implies that the resolution is not responsible for the changes of summer blocking. Another possible reason is that the LSI-double-jets-blocking positive feedback is weaker or missing in the simulations. Although the models have large uncertainty in the trend of summer blocking, most of models capture that the decreases of summer blocking between RCPs and historical runs are less than that in winter except for ACCESS1-0, CMCC-CM, GFDL-ESM2M, IPSL-CM5B-LR, MIROC5, MRI-CGCM3. The trend of winter and summer blocking changes and LSI changes simulating from the IPSL-CM5A-LR and MIROC-ESM-CHEM model are consistent with observations. Under RCP8.5, the winter LSI has a significant increase, which is much more than that in summer. The ensemble mean of blocking changes and LSI changes are stronger than that in the RCP4.5 experiment. Consistent with our analysis, the sensitivity of winter

Fig. 12 Averaged changes in LSI (K) and blocking days between picontrol and 1pctco2 experiments (1pctco2 minus picontrol) from the 20-year (year 120–139) simulations of 12 models. Small crosses overlaying every marker indicate the 0.1 standard deviation of the corresponding model. Red large crosses are 12 models ensemble means and ±1 standard deviation and blue large crosses are the ensemble means from high resolution (<2°) models (CCSM4, MIROC5, MPI-ESM-LR, MRI-CGCM3)

structure provides a narrow tunnel with reduced westerly environment, which can increase the appearance of blocking by trapping the free synoptic waves with zonal wave number $k = 6$–8. Especially, during extreme high LSI in summer, this mechanism supports a strong magnification of planetary wave amplitudes through resonance and extends the periods of summer extremes. On the other way, the increasing summer LSI also stimulates more transient waves activities and does not decrease the background westerly wind between double jets, which make the blocking have a rapid

retrogression and less duration. Results of the composite analysis presenting in Sect. 5 show that the summer blocking numbers are strongly related to the LSI phase. During the positive phase, the total blocking event number increases from 69 to 79, which is possibly caused by LSI-double-jets-blocking positive feedback (Petoukhov's theory). But in positive phase of summer LSI, average duration decreases more than 0.7 days and long blocking duration decreases 2.6 days compared to negative phase, which is mainly controlled

by LSI-transient-waves-blocking negative feedback (Luo's theory).

Comparing the winter and summer feedback between blocking and LSI as shown in Fig. 9, there are four factors limiting the response of summer blocking. First one is the opposite effect between LSI-transient-waves-blocking negative feedback and LSI-double-jets-blocking positive feedback. The second one is the sensitivity of stationary waves to LSI, Fig. 10b, e suggest that stationary waves changes due to LSI changes in summer are much less than winter, which implies that the summer blocking and westerly has a low sensitivity to land-sea thermal contrast. The third one is the limit of double-jet structure. When summer LSI is positive anomaly but not enough large to induce the appearance of a double-jet structure, the magnification effect of planetary waves on the blocking is very small. The fourth one is the impact of Arctic sea ice loss. With rapid Arctic warming, sea ice loss has induced a negative AO-type circulation with significant cooling trends over midlatitudes. Therefore, sea ice loss has a negative contribution to an increase in the land-sea thermal contrast and reduces the probability of summer blocking. However, the sensitivity of summer blocking will rapidly increase when sea ice in Arctic completely disappears, then summer warming trend will be also much higher than present.

The above analysis suggests that the sensitivity of summer blocking should be lower than winter, which contradicts with observations in Fig. 9. However, the positive feedback in summer and winter discussed in this study are based on the zonal asymmetric thermal forcing. As suggested by Huang et al. (2016a), the blocking is influenced by the combination of zonal thermal forcing (ZTF) and meridional thermal forcing (MTF). In summer, the MTF associated with sea ice loss has a negative contribution to the sensitivity of blocking (Wu et al. 2016). In winter, the rapidly sea ice loss drives a "Warm Arctic, Cold Eurasian (WACE)" pattern, which induce more extreme cold weather over midlatitude (Cohen et al. 2013, 2014; Huang et al. 2016a; Luo et al. 2016; Zhang et al. 2016). The quantitative analysis of MTF and ZTF is highly controversial and need further investigation. However, the recent study pointed out that the arctic sea ice loss is responsible for "Warm Arctic" but not for "Cold Continents" (Sun et al. 2016), which implies that the MTF associated with sea ice loss has a less, even no, influence on midlatitude blocking. Figure 13 shows a diagram scheme to explain the influence of ZTF and MTF on blocking sensitivity. It is worth noting that ZTF indicates the zonal thermal contrast, which is consistent with the absolute values of winter LSI. Therefore, the ZTF decreases with LSI increasing in winter. Consistently, the sensitivity of blocking associated with ZTF in winter is larger than summer and the MTF decreases the sensitivity of blocking in both winter and
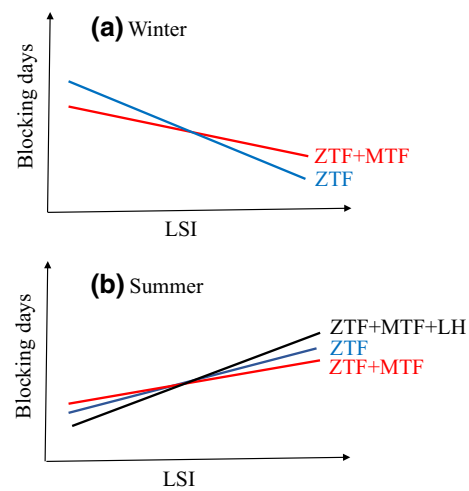

Fig. 13 The diagram scheme of blocking sensitivity to LSI impacted by zonal thermal forcing (ZTF) and meridional thermal forcing (MTF)

summer. Latent heat release, sensible heat and radiative heat, the possible impact factors for blocking changes, may fill the gap between predicted and observational sensitivity of winter and summer blocking. The latent heat release has an important role in ascending air for blocking. Pfahl et al. (2015) pointed out that 30–45% of the air involved in NH blocking are heated by more than 2K before they arrive in the blocking system. Because the water vapor has increased with enhanced warming in air temperature in global scale, the latent heat might play a more important role than before for blocking formation and maintenance. The projections of blocking changes in the future should consider the latent heat changes. Although this paper investigates how the land-sea thermal contrast affects the blocking duration through changing the background conditions, the details of the life cycle of blocking events can not be reflected by the used theory model. Therefore, some moderate complex models, such as Luo et al. (2014a, b), are needed to describe the prolonging or shortening of the blocking duration by the land-sea thermal contrast.

References

Andrews DG, Holton JR, Leovy CB (1987) Middle atmosphere dynamics. Academic press, San Francisco, pp 489

Arai M, Kimoto M (2008) Simulated interannual variation in summertime atmospheric circulation associated with the East Asian monsoon. Clim Dyn 31:435–447. doi:10.1007/s00382-007-0317-y

Charney JG, DeVore JG (1979) Multiple flow equilibria in the atmosphere and blocking. J Atmos Sci 36:1205–1216

Chen W, Yang S, Huang RH (2005) Relationship between stationary planetary wave activity and the East Asian winter monsoon. J Geophys Res D Atmos 110:1–12. doi:10.1029/2004JD005669

Cohen J (2016) An observational analysis: tropical relative to Arctic influence on midlatitude weather in the era of Arctic amplification. Geophys Res Lett 43:5287–5294. doi:10.1002/2016GL069102

Cohen J, Jones J, Furtado JC, Tziperman E (2013) Warm Arctic, cold continents: a common pattern related to Arctic sea ice melt, snow advance, and extreme winter weather. Oceanography 26:150–160. doi:10.5670/oceanog.2013.70

Cohen J, Screen J a., Furtado JC et al (2014) Recent Arctic amplification and extreme mid-latitude weather. Nat Geosci 7:627–637. doi:10.1038/ngeo2234

Dole R, Hoerling M, Perlwitz J et al (2011) Was there a basis for anticipating the 2010 Russian heat wave? Geophys Res Lett 38:1–5. doi:10.1029/2010GL046582

Dong B, Gregory JM, Sutton RT (2009) Undestanding land-sea warming contrast in response to increasing greenhouse gases. Part I: Transient adjustment. J Clim 22:3079–3097. doi:10.1175/2009JCLI2652.1

Dunn-Sigouin E, Son S-w (2013) Northern Hemisphere blocking frequency and duration in the CMIP5 models. J Geophys Res 118:1179–1188

Egger J (1978) Dynamics of blocking highs. J Atmos Sci 35:1788–1801. doi:10.1175/1520-0469(1978)035<1788:DOBH>2.0.CO;2

Fu Q, Johanson CM, Wallace JM, Reichler T (2006) Enhanced midlatitude tropospheric warming in satellite measurements. Science 312:1179–1179. doi:10.1126/science.1125566

Grise K, Polvani L (2014) The response of midlatitude jets to increased CO2: distringuishing the roles of sea surface temperature and direct radiative forcing. Geophys Res Lett 41:6863–6871. doi:10.1002/2014GL061638

Guan X, Huang J, Guo R et al (2015a) Role of radiatively forced temperature changes in enhanced semi-arid warming over East Asia. Atmos Chem Phys 15:22975–23004. doi:10.5194/acpd-15-22975-2015

Guan X, Huang J, Guo R, Lin P (2015b) The role of dynamically induced variability in the recent warming trend slowdown over the Northern Hemisphere. Sci Rep 5:12669. doi:10.1038/srep12669

Hansen J, Ruedy R, Sato M, Lo K (2010) Global surface temperature change. Rev Geophys 48:RG4004. doi:10.1029/2010RG000345

He Y, Huang J, Ji M (2014) Impact of land–sea thermal contrast on interdecadal variation in circulation and blocking. Clim Dyn 43:3267–3279. doi:10.1007/s00382-014-2103-y

Huang J, Guan X, Ji F (2012) Enhanced cold-season warming in semi-arid regions. Atmos Chem Phys 12:5391–5398

Huang J, Xie Y, Guan X et al (2016a) The dynamics of the warming hiatus over the Northern Hemisphere. Clim Dyn 48:429. doi:10.1007/s00382-016-3085-8

Huang J, Yu H, Guan X et al (2016b) Accelerated dryland expansion under climate change. Nat Clim Chang 6:166–171. doi:10.1038/nclimate2837

Inoue J, Hori ME, Takaya K (2012) The role of barents sea ice in the wintertime cyclone track and emergence of a warm-Arctic cold-Siberian anomaly. J Clim 25:2561–2569. doi:10.1175/JCLI-D-11-00449.1

Ji F, Wu Z, Huang J, Chassignet EP (2014) Evolution of land surface air temperature trend. Nat Clim Chang 4:462–466

Joshi MM, Gregory JM, Webb MJ et al (2008) Mechanisms for the land/sea warming contrast exhibited by simulations of climate change. Clim Dyn 30:455–465. doi:10.1007/s00382-007-0306-1

Kaas E, Branstator G (1993) The relationship between a zonal index and blocking activity. J Atmos Sci 50:3061–3077. doi:10.1175/1520-0469(1993)050<3061:TRBAZI>2.0.CO;2

Kalnay E, Kanamitsu M, Kistler R et al. (1996) The NCEP/NCAR 40-year reanalysis project. Bull Am Meteorol Soc 77:437–471. doi:10.1175/1520-0477(1996)077<0437:TNYRP>2.0.CO;2

Kamae Y, Watanabe M, Kimoto M, Shiogama H (2014a) Summertime land–sea thermal contrast and atmospheric circulation over East Asia in a warming climate—part I: past changes and future projections. Clim Dyn 43:2553–2568. doi:10.1007/s00382-014-2073-0

Kamae Y, Watanabe M, Kimoto M, Shiogama H (2014b) Summertime land–sea thermal contrast and atmospheric circulation over East Asia in a warming climate—part II: Importance of CO$_2$-induced continental warming. Clim Dyn 43:2569–2583. doi:10.1007/s00382-014-2146-0

Kawatani Y, Hamilton K, Noda A (2012) The effects of changes in sea surface temperature and CO$_2$ concentration on the quasibiennial oscillation. J Atmos Sci 69:1734–1749. doi:10.1175/JAS-D-11-0265.1

Kobayashi S, Ota Y, Harada Y et al (2015) The JRA-55 reanalysis: general specifications and basic characteristics. J Meteorol Soc Japan Ser II 93:5–48. doi:10.2151/jmsj.2015-001

Kosaka Y, Xie S-P (2013) Recent global-warming hiatus tied to equatorial Pacific surface cooling. Nature 501:403–407. doi:10.1038/nature12534

Li J, Wang J (2003) A modified zonal index and its physical sense. Geophys Res Lett

Li C, Stevens B, Marotzke J (2015) Eurasian winter cooling in the warming hiatus of 1998–2012. Geophys Res Lett 42:8131–8139. doi:10.1002/2015GL065327

Luo D, Yao Y, Feldstein SB (2014a) Regime transition of the North Atlantic oscillation and the extreme cold Event over Europe in January–February 2012. Mon Weather Rev 142:4735–4757. doi:10.1175/MWR-D-13-00234.1

Luo D, Cha J, Zhong L, Dai A (2014b) A nonlinear multiscale interaction model for atmospheric blocking: the eddy-blocking matching mechanism. Q J R Meteorol Soc 140:1785–1808. doi:10.1002/qj.2337

Luo D, Xiao Y, Yao Y et al (2016) Impact of ural blocking on winter warm Arctic–cold Eurasian anomalies. part I: blocking-induced amplification. J Clim 29:3925–3947. doi:10.1175/JCLI-D-15-0611.1

Luo D, Yao Y, Dai A et al (2017a) Increased quasi-stationarity and persistence of winter ural blocking and Eurasian extreme cold events in response to Arctic warming. part I: insights from observational analyses. J Clim. doi:10.1175/JCLI-D-16-0261.1

Luo D, Yao Y, Dai A et al (2017b) Increased quasi-stationarity and persistence of winter ural blocking and Eurasian extreme cold events in response to arctic warming. part II: a theoretical explanation. J Clim. doi:10.1175/JCLI-D-16-0262.1

Masato G, Hoskins BJ, Woollings TJ (2012) Wave-breaking characteristics of midlatitude blocking. Q J R Meteorol Soc 138:1285–1296. doi:10.1002/qj.990

Masato G, Hoskins BJ, Woollings T (2013) Winter and summer Northern hemisphere blocking in CMIP5 models. J Clim 26:7044–7059. doi: 10.1175/JCLI-D-12-00466.1

Mitchell TD, Jones PD (2005) An improved method of constructing a database of monthly climate observations and associated high-resolution grids. Int J Climatol 25:693–712. doi: 10.1002/joc.1181

Molnos S, Mamdouh T, Petri S et al (2017) A network-based detection scheme for the jet stream core. Earth Syst Dyn 8:75–89. doi: 10.5194/esd-8-75-2017

Molteni F, King MP, Kucharski F, Straus DM (2011) Planetary-scale variability in the northern winter and the impact of land-sea thermal contrast. Clim Dyn 37:151–170. doi: 10.1007/s00382-010-0906-z

Mori M, Watanabe M, Shiogama H et al (2014) Robust Arctic sea-ice influence on the frequent Eurasian cold winters in past decades. Nat Geosci 7:869–874. doi: 10.1038/ngeo2277

Morice CP, Kennedy JJ, Rayner NA, Jones PD (2012) Quantifying uncertainties in global and regional temperature change using an ensemble of observational estimates: the HadCRUT4 data set. J Geophys Res Atmos 117:1–22. doi: 10.1029/2011JD017187

Nakamura H, Fukamachi T (2004) Evolution and dynamics of summertime blocking over the Far East and the associated surface Okhotsk high. Q J R Meteorol Soc 130:1213–1233. doi:10.1256/qj.03.101

Nakamura H, Nakamura M, Anderson JL (1997) The Role of high- and low-frequency dynamics in blocking formation. Mon Weather Rev 125:2074–2093. doi:10.1175/1520-0493

Ogi M, Yamazaki K, Tachibana Y (2004) The summertime annular mode in the Northern Hemisphere and its linkage to the winter mode. J Geophys Res D Atmos 109:1–15. doi:10.1029/2004JD004514

Ogi M, Yamazaki K, Tachibana Y (2005) The summer northern annular mode and abnormal summer weather in 2003. Geophys Res Lett 32:1–4. doi:10.1029/2004GL021528

Otto FEL, Massey N, Van Oldenborgh GJ et al (2012) Reconciling two approaches to attribution of the 2010 Russian heat wave. Geophys Res Lett 39:1–5. doi:10.1029/2011GL050422

Petoukhov V, Rahmstorf S, Petri S, Joachim H (2013) Quasiresonant amplification of planetary waves and recent Northern Hemisphere weather extremes. Proc Natl Acad Sci. doi:10.1073/pnas.1222000110

Petoukhov V, Petri S, Rahmstorf S et al (2016) Role of quasiresonant planetary wave dynamics in recent boreal spring-to-autumn extreme events. Proc Natl Acad Sci 113:6862–6867. doi:10.1073/pnas.1606300113

Pfahl S, Schwierz C, Croci-Maspoli M et al (2015) Importance of latent heat release in ascending air streams for atmospheric blocking. Nat Geosci 8:610–614. doi:10.1038/ngeo2487

Rahmstorf S, Coumou D (2011) Increase of extreme events in a warming world. Proc Natl Acad Sci 108:17905–17909. doi:10.1073/pnas.1101766108

Rayner NA, Parker DE, Horton EB et al (2003) Global analyses of sea surface temperature, sea ice, and night marine air temperature since the late nineteenth century. J Geophys Res. doi:10.1029/2002JD002670

Rikus L (2015) A simple climatology of westerly jet streams in global reanalysis datasets part I: mid latitude upper tropospheric jets, Clim Dynam. doi:10.1007/s00382-015-2560-y

Scaife AA, Woollings T, Knight J et al (2010) Atmospheric blocking and mean biases in climate models. J Clim 23:6143–6152. doi:10.1175/2010JCLI3728.1

Seneviratne SI, Donat MG, Mueller B, Alexander LV (2014) No pause in the increase of hot temperature extremes. Nat Clim Chang 4:161–163. doi: 10.1038/nclimate2145

Shabbar A, Huang J, Higuchi K (2001) The relationship between the wintertime North Atlantic oscillation and blocking episodes in the North Atlantic. Int J Climatol 21:355–369. doi:10.1002/joc.612

Shaw T, Voigt A (2015) Tug of war on summertime circulation between radiative forcing and sea surface warming. Nature Geosci 8:560–566. doi:10.1038/NGEO2449

Shutts GJ (1983) The propagation of eddies in diffluent jetstreams : eddy vorticity forcing of' blocking' flow fields. Q J R Meteorol Soc 737–761. doi:10.1002/qj.49710946204

Sillmann J, Donat MG, Fyfe JC, Zwiers FW (2014) Observed and simulated temperature extremes during the recent warming hiatus. Environ Res Lett 9:064023. doi:10.1088/1748-9326/9/6/064023

Stott PA, Stone DA, Allen MR (2004) Human contribution to the European heatwave of 2003. Nature 432:610–614. doi:10.1038/nature03089

Sun L, Perlwitz J, Hoerling M (2016) What caused the recent "Warm Arctic, cold continents" trend pattern in winter temperatures?. Geophys Res Lett 5345–5352. doi:10.1002/2016GL069024

Sutton RT, Dong B, Gregory JM (2007) Land/sea warming ratio in response to climate change: IPCC AR4 model results and comparison with observations. Geophys Res Lett 34:2–6. doi:10.1029/2006GL028164

Tachibana Y, Nakamura T, Komiya H, Takahashi M (2010) Abrupt evolution of the summer Northern Hemisphere annular mode and its association with blocking. J Geophys Res Atmos 115:1–13. doi :10.1029/2009JD012894

Taylor KE, Stouffer RJ, Meehl G a. (2012) An overview of CMIP5 and the experiment design. Bull Am Meteorol Soc 93:485–498. doi:10.1175/BAMS-D-11-00094.1

Tibaldi S, Molteni F (1990) On the operational predictability of blocking. Tellus A 42:343–365. doi:10.1034/j.1600-0870.1990.t01-2-00003.x

Trenberth K, Fasullo J, Branstator G, Philips A (2014) Seasonal aspects of the recent pause in surface warming. Nat Clim Chang 4:911–916. doi:10.1038/nclimate2341

Tung KK, Lindzen RS (1979) A theory of stationary long waves. part I: a simple theory of blocking. Mon Weather Rev 107:714–734. doi:10.1175/1520-0493

Tyrlis E, Hoskins BJ (2008) Aspects of a Northern hemisphere atmospheric blocking climatology. J Atmos Sci 65:1638–1652. doi:10.1175/2007JAS2337.1

Wallace JM, Fu Q, Smoliak BV et al (2012) Simulated versus observed patterns of warming over the extratropical Northern hemisphere continents during the cold season. Proc Natl Acad Sci 109:14337–14342

Wallace JM, Zhang Y, Bajuk L (1996) Interpretation of interdecadal trends in Northern Hemisphere surface air temperature. J Clim 9:249–259. doi:10.1175/1520-0442(1996)009<0249:IOITIN>2.0.CO;2

Wu Q, Straus DM (2004) AO, COWL, and observed climate trends. J Clim 17:2139–2156. doi:10.1175/1520-0442(2004)017<2139:ACAOCT>2.0.CO;2

Wu Q, Cheng L, Chan D et al (2016) Suppressed midlatitude summer atmospheric warming by Arctic sea ice loss during 1979–2012. Geophys Res Lett 43:2792–2800. doi:10.1002/2016GL068059

Yamazaki A, Itoh H (2013) Vortex–Vortex interactions for the maintenance of blocking. Part I: the selective absorption mechanism and a case study. J Atmos Sci 70:725–742. doi:10.1175/JAS-D-11-0295.1

Zhang J, Tian W, Chipperfield MP et al (2016) Persistent shift of the Arctic polar vortex towards the Eurasian continent in recent decades. Nat Clim Chang 6:1094–1099. doi:10.1038/nclimate3136

Zhu Z, Zhu B (1982) The nonlinear equilibrium states of ultra-long waves induced by zonal asymmetric thermal forcing and blocking situation. Sci Sinica 25:1201–1212 (Chinese).